(32) The reason why the peak intensity of the Tyr $C_\beta$ signal is so low is at present not clear. However, it is probable that such a loss of peak intensity is associated with the presence of molecular motion at the Larmor frequency of the rotating frame corresponding to the amplitude of the proton decoupling field (VanderHart, D. L.; Earl, W. L.; Garroway, A. N. *J. Magn. Reson.* **1981**, *44*, 361). It is also pointed out that no appreciable Tyr $C_\beta$ signal was observed due to freezing of such motion at a temperature of 226 K, whereas the peak intensity of the Ala $C_\beta$ signal was substantially decreased owing to the partial freezing of the $C_3$ rotation (Ishida, M. MS thesis, Tokyo University of Agriculture and Technology, 1989).
(33) Saitô, H.; Yokoi, M.; Aida, M.; Kodama, M.; Oda, T.; Sato, Y. *Magn. Reson. Chem.* **1988**, *26*, 155.
(34) Schaefer, J.; Stejskal, E. O.; Buchdahl, R. *Macromolecules* **1977**,*10*, 384.
(35) Pople, J. A.; Scheider, W. G.; Bernstein, H. J. *High-resolution Nuclear Magnetic Resonance*; McGraw-Hill: New York, 1959.
(36) Saitô, H.; Tabeta, R. In *Peptide Chemistry 1987*; Shiba, T., Sakakibara, S., Eds.; Protein Research Foundation: Osaka, 1988; pp 53.
(37) Saitô, H.; Tabeta, R.; Yokoi, M. *Magn. Reson. Chem.* **1988**, *26*, 775.
(38) The $C_\zeta$ signal is also not resolved from the $C_\delta$ and $C_\epsilon$ signals.
(39) Measurements of Tyr $C_\epsilon$ in fibroin samples were not easy because of lower amino acid composition (ca. 4%) and accidential overlap with sidebands from an intense carbonyl signal. The $^{13}C$ $T_1^C$ value of lyophilized silk II sample turned out to be on the order of 28 s. This finding indicates that the Tyr residue in fibroin is located in an environment of a more packed state than in $(Tyr)_n$. In fact, the rate of flip-flop motion of this sample, if any, is much longer than $10^{-8}$ s but shorter than $10^{-2}$ s.
(40) This sort of deflection in the peak intensity of $(Ser)_n$ is not ascribed to any instrumental artefact because there exists no such deflection in the similar plot of Ala $C_\beta$ whose $T_1^C$ is of the same magnitude with that of Ser $C_\beta$.
(41) Janin, J.; Wodak, S.; Levit, M.; Maigret, B. *J. Mol. Biol.* **1978**, *125*, 357.
(42) Gray, T.; Matthews, B. W. *J. Mol. Biol.* **1984**, *175*, 75.
(43) Asakura, T.; Yamaguchi, T. *J. Serc. Soc. Jpn.* **1987**, *56*, 300.
(44) Ishida, M.; Asakura, T.; Yokoi, M.; Saitô, H. *Macromolecules*, following paper in this issue.

# Solvent- and Mechanical-Treatment-Induced Conformational Transition of Silk Fibroins Studied by High-Resolution Solid-State $^{13}C$ NMR Spectroscopy

**Mika Ishida,† Tetsuo Asakura,† Motoko Yokoi,‡ and Hazime Saitô*,‡**

*Faculty of Technology, Tokyo University of Agriculture and Technology, Nakamachi 2-chome, Koganei, Tokyo, Japan, and Biophysics Division, National Cancer Center Research Institute, Tsukiji 5-chome, Chuo-ku, Tokyo, Japan.* *Received November 29, 1988; Revised Manuscript Received April 5, 1989*

ABSTRACT: We have recorded $^{13}C$ NMR spectra of silk fibroins from *Bombyx mori* and *Philosamia cynthia ricini* to examine solvent- (or diluent-) or mechanical-treatment-induced conformational transition. First, $^{13}C$ NMR spectra of silk I and II forms of the crystalline (Cp) fraction of *B. mori* fibroin and of $\alpha$-helix and $\beta$-sheet forms of *P. c. ricini* fibroin were recorded under improved spectral resolution than those previously reported. For the latter fibroin, two kinds of $\alpha$-helical domains (stable and less stable $\alpha$-helical domains consisting of longer and shorter Ala sequences, respectively) were distinguished in view of the substantial difference in the stability of helices between the solid and the solution. Hydration of *B. mori* fibroin resulted in a stabilization of silk I forms, as manifested from the significant narrowing of peaks without inducing conformational transition. In *P. c. ricini* fibroin, however, hydration caused a partial conformational change from the less stable $\alpha$-helix to the $\beta$-sheet form, without any change in line widths. Furthermore, solvent-induced conformational change of *B. mori* fibroin from the "random coil" to the silk II form was examined and explained in terms of ease of dehydration by the solvent used. In addition, conformational change by mechanical treatments such as drawing and compression was also examined.

## Introduction

Crystalline silk fibroins are known to exist in one of the polymorphs, either silk I or silk II and either $\alpha$-helix or $\beta$-sheet forms, depending on the species of silkworms, *Bombyx mori* and *Philosamia cynthia ricini*, respectively.[1-4] Besides, the "random coil" form can be distinguished from the above-mentioned polymorphs in fibroins of noncrystalline samples. Previous works showed that a number of solvents (or diluents) or mechanical treatments induce conformational transition from the less stable "random coil" or silk I form to the more stable silk II ($\beta$-sheet) form.[5-7] Extensive study of such a process is very important to gain a better understanding of the relative stability of the respective forms as well as a plausible mechanism of induced conformational transition.

Recently, Asakura and co-workers attempted to utilize this sort of conformational transition of silk fibroins to develop an immobilized enzyme support system without inducing inactivation of entrapped enzymes.[8-11] Here, entrapment is facilitated by the partial formation of effective physical "cross-links" of polymers from aggregates of ordered $\beta$-sheet sequences. Effectiveness of this procedure is based on the fact that such conformational transition is induced by a gentle process such as solvent or mechanical treatment. For this purpose, it is important to clarify and to control various types of conformational

† Tokyo University of Agriculture and Technology.
‡ National Cancer Center Research Institute.

0024-9297/90/2223-0088$02.50/0 

transitions of fibroins in a more detailed manner.[8]

Traditional means of conformational elucidation such as X-ray diffraction or infrared spectroscopy, however, is not always adequate for this purpose because these methods are not suitable for the quantitative evaluation of the relative proportion of noncrystalline forms. In this connection, we have demonstrated that a high-resolution solid-state $^{13}C$ NMR study[12-14] is a very useful means to evaluate the relative proportion of several types of forms, even if they are mixed in a sample. This is based on the fact that the three forms of silk fibroins including "random coil" are readily distinguished by examination of the conformation-dependent $^{13}C$ chemical shifts of the respective amino acid residues as determined by the high-resolution solid-state NMR method. In fact, the $^{13}C$ chemical shifts of respective amino acid residues are independent of its sequence and are mainly determined by local conformations determined by the torsion angles ($\phi$, $\psi$) and the manner of hydrogen bonding.[15-17]

In this paper, we first recorded $^{13}C$ NMR spectra of highly crystalline samples under improved spectral resolution as a reference for the study of conformational modification. Then, we analyzed the effect of hydration of fibroin on the stability of respective forms or induced conformational transition as studied by high-resolution solid-state $^{13}C$ NMR spectroscopy. Furthermore, we studied conformational transition of a variety of fibroin samples by means of solvent or mechanical treatment. The starting materials used in this study are as follows: (a) cast film, (b) regenerated fibroin solution, (c) lyophilized fibroin, and (d) fibroin gel.

## Experimental Section

**Materials. *B. mori* Fibroin.** Preparation of the degummed fibroin and the crystalline (Cp) fraction was described in the preceding paper.[18,19] The dried degummed fibroins were dissolved in 9 M LiBr aqueous solution (3% w/v) at 40 °C, followed by dialysis against distilled water (regenerated fibroin solution). The cast film was obtained by casting the regenerated fibroin solution on a PMMA plate, followed by drying. Lyophilized fibroin was obtained from the regenerated fibroin solution. Fibroin gel was a product of prolonged dialysis (4 days). These starting materials (regenerated fibroin solution, lyophilized fibroin, and fibroin gel) were mixed or immersed in organic solvent while vigorously stirred (0.5 h for the regenerated solution or the fibroin gel; 1 week for the lyophilized fibroin).

The cast film was used as a starting material and was prepared by the following three kinds of methods.[20,21] Samples were hydrated by placing in a desiccator of 96% relative humidity (RH) for 30 min prior to the following mechanical treatments. The hydrate sample was then compressed at 560 kg/cm$^2$ for 20 min to obtain the compressed film. Second, the hydrate film was uniaxially drawn 3-fold by placing it on a stretcher for 10 min (the rate of drawing was 0.2 mm/s). Third, the fibroin film was kept under 20 °C, 96% RH for 1 week without any mechanical treatment.

***P. c. ricini* Fibroins.** $\alpha$-Helical *P. c. ricini* fibroin was obtained by casting liquid silk directly taken from the posterior silk gland of the mature larva on a PMMA plate.[18] Highly crystalline $\beta$-sheet fibroin was prepared from precipitates of *P. c. ricini* fibroin digested by chymotrypsin.[22] The cast film of *P. c. ricini* fibroin was prepared following the same preparation of the cast film from *B. mori* fibroin, and the resulting hydrated film was compressed or drawn as described above.

The 75.46-MHz high-resolution solid-state $^{13}C$ NMR spectra were recorded on a Bruker CXP-300 spectrometer equipped with an accessory of cross polarization–magic angle spinning (CP-MAS). The detailed conditions of data acquisition were the same as those described in the preceding paper.[18] Except for the well-hydrated samples, all samples were dried in vacuo overnight prior to NMR measurements. The well-hydrated samples were prepared by placing the sample in a 96% RH desiccator for 15–45 h. The $^{13}C$ chemical shifts were calibrated through the external carboxyl peak of glycine (176.03 ppm) and converted to the values from tetramethylsilane ($Me_4Si$).

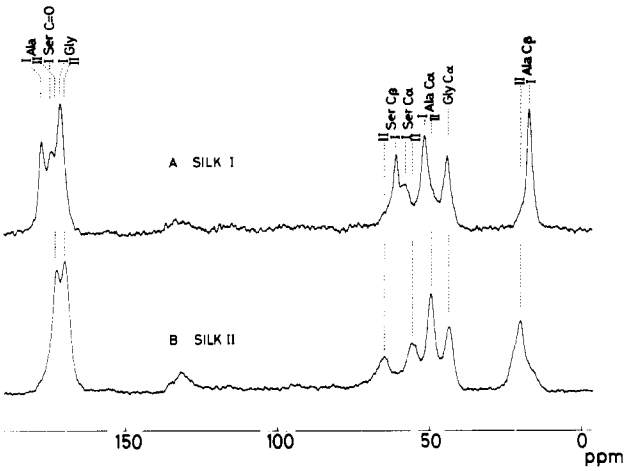


**Figure 1.** 75.46-MHz $^{13}C$ NMR spectra of silk fibroins from the Cp fraction of *B. mori* fibroin adopting silk I (A) and silk II (B) forms in the solid state. Roman letters I and II above the peaks stand for the peak positions from silk I and silk II, respectively.

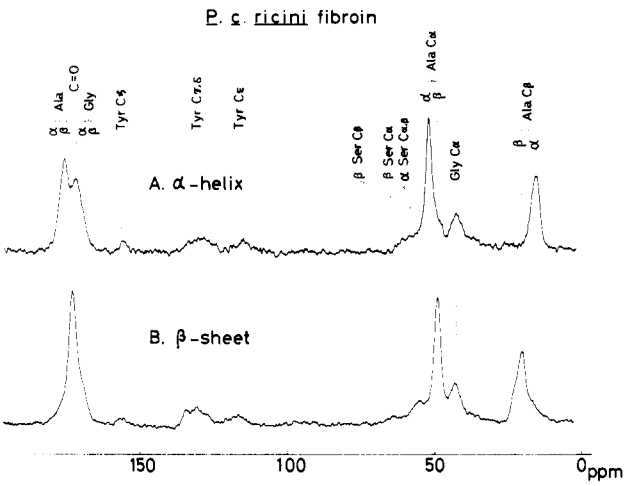


**Figure 2.** 75.46-MHz $^{13}C$ NMR spectra of $\alpha$-helix (A) and $\beta$-sheet (B) forms from *P. c. ricini* fibroin in the solid state. The greek letters $\alpha$ and $\beta$ stand for the peaks from the $\alpha$-helix and $\beta$-sheet forms.

## Results

Figure 1 demonstrates the $^{13}C$ NMR spectra of silk I (Figure 1A) and silk II (Figure 1B) forms of the Cp fraction whose spectral resolution is much better than that in previous work.[12-14,23,24] In particular, the achieved spectral resolution in the silk I sample is noteworthy;[25] the carbonyl peaks are resolved into three regions (Figure 1A) in which the uppermost and the lowermost signals are in accordance with the $^{13}C$ NMR signals of Gly and Ala residues in form II of $(Ala\text{-}Gly)_n$,[13] respectively. The remaining least intense central peak is thus readily ascribed to the Ser C=O signal by taking into account the relative proportion of amino acid residues. Then, the upper and lower carbonyl peaks of the silk II sample (Figure 1B) are ascribed to Gly and Ala plus Ser residues, respectively, on the basis of the relative proportion of amino acid residues and of the $^{13}C$ chemical shifts of the reference samples: form I ($\beta$-sheet) of $(Ala\text{-}Gly)_n$ and the $\beta$-sheet form of $(Ser)_n$.[13] Figure 2, parts A and B, demonstrates $^{13}C$ NMR signals of $\alpha$-helix and $\beta$-sheet forms of *P. c. ricini* fibroin, respectively. Again, the carbonyl sig-

Table I
$^{13}C$ Chemical Shifts of Polymorphic Forms of Silk Fibroins and Related Polypeptides (ppm from $Me_4Si$)

| | silk I | | silk II | | α-helix | | β-sheet | |
|---|---|---|---|---|---|---|---|---|
| | *B. mori* | ref polypeptides | *B. mori* | ref polypeptides | *P. c. ricini* | ref polypeptides | *P. c. ricini* | ref polypeptides |
| Ala $C_\alpha$ | 51.4 | 50.5[a] | 49.4 | 48.5[b] | 52.5 | 52.4[c] | 48.6 | 48.2[d] |
| $C_\beta$ | 16.5 | 16.6[a] | 20.2 | 20.0[b] | 15.7 | 14.9[c] | 20.0 | 19.9[d] |
| C=O | 177.0 | 177.1[a] | 172.3 | 171.9[b] | 176.2 | 176.4[c] | 171.8 | 171.8[d] |
| Gly $C_\alpha$ | 43.8 | 43.7[a] | 43.1 | 43.3[b] | 43.0 | | 42.8 | 43.2[i] |
| C=O | 170.7 | 171.9[a] | 169.5 | 169.2[b] | 172.3 | 171.7[h] | 168.8 | 168.4[i] |
| Ser $C_\alpha$ | 58.0 | | 55.4 | 54.4[f] | [g] | | 54.2 | 54.4[f] |
| $C_\beta$ | 60.7 | | 63.6 | 63.9[f] | [g] | | 63.0 | 63.9[f] |
| C=O | 173.7 | | 172.3[e] | 171.2[f] | [g] | | 171.8[j] | 171.2[f] |

[a] $(Ala\text{-}Gly)_n$ II.[13] [b] $(Ala\text{-}Gly)_n$ I.[13] [c] $(Ala)_n$, α-helix form.[31] [d] $(Ala)_n$, β-sheet form.[31] [e] Superimposed on the Ala C=O peak. [f] $(Ser)_n$, β-sheet form.[13] [g] Not defined. [h] (Ala,Gly*)$_n$, random copolymer, 5% Gly* ([1-$^{13}C$]Gly).[32] [i] $(Gly)_n$, β-sheet form.[31] [j] Superimposed on the Ala C=O peak.

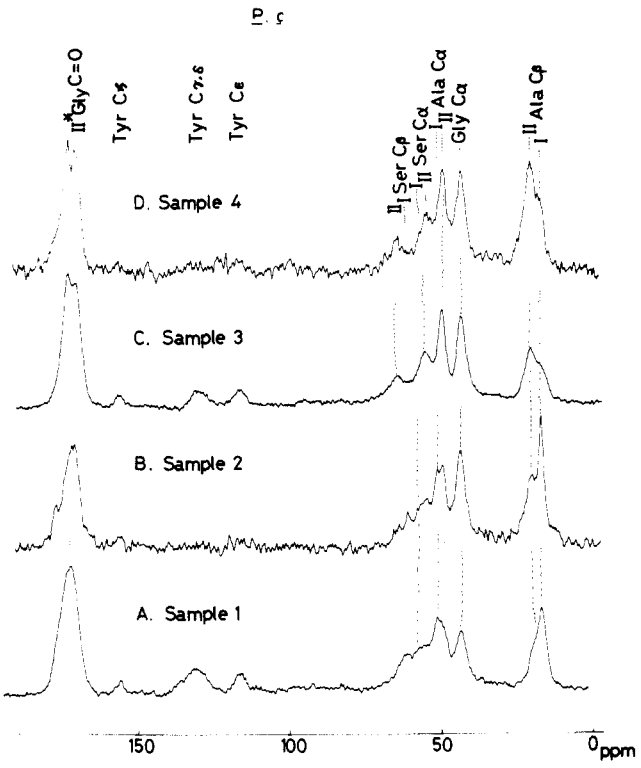


Figure 3. 75.46-MHz $^{13}C$ NMR spectra of anhydrous (samples 1 and 3) and hydrate (96% RH; 15–45 h; samples 2 and 4) samples from *B. mori* fibroin: sample 1, cast film; sample 2, hydrated sample 1; sample 3, lyophilized fibroin after mixing fibroin solution in methanol solution; sample 4, hydrated sample 3. The peak with an asterisk in the carbonyl region stands for the Ala C=O peak of silk II and the Ala and Gly C=O peaks of the silk I form.

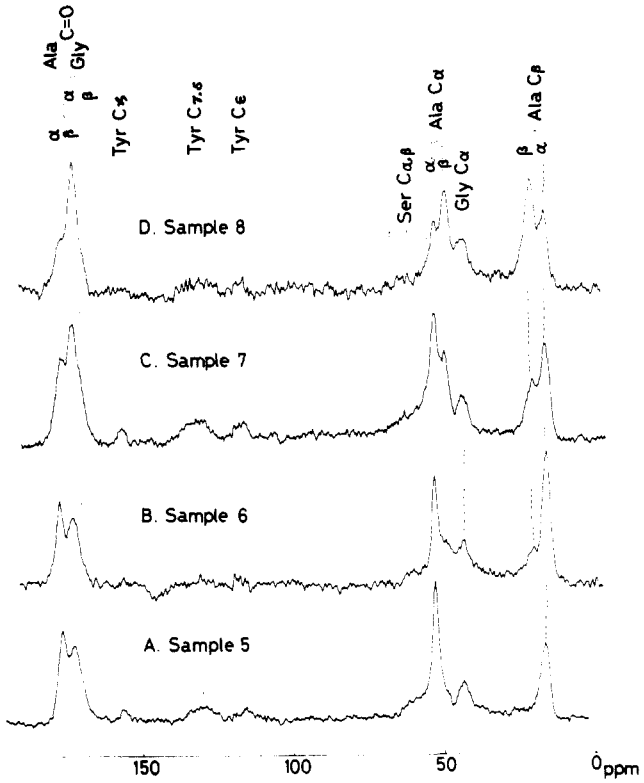


Figure 4. 75.46-MHz $^{13}C$ NMR spectra of anhydrous (samples 5 and 7) and hydrate (96% RH; 15–45 h; samples 6 and 8) fibroin samples from *P. c. ricini* in the solid state: sample 5, cast film; sample 6, hydrated sample 5; sample 7, cast film containing a large proportion of the β-sheet form; sample 8, hydrated sample 7.

nal that arose from a broad singlet in the previous work[13] is now resolved into a doublet signal (Figure 2A). The lower and upper signals are readily ascribed to Ala and Gly $^{13}C$ signals, by taking into account the relative proportion of amino acid composition and the peak position of the reference compounds (see Table I). The carbonyl peak of the Gly residue in the β-sheet form, however, is not resolved but appears at a shoulder of the intense Ala C=O signal. The peak positions of Ser $C_\alpha$ and $C_\beta$ are not clearly resolved as compared with those of the β-sheet form. The $^{13}C$ chemical shifts thus obtained were summarized in Table I.

Figures 3 and 4 summarize the effect of hydration on the $^{13}C$ NMR spectra of *B. mori* and *P. c. ricini* fibroins, respectively. Hydration of the former fibroins resulted in a substantial narrowing of the $^{13}C$ NMR signals of the silk I form, whereas the effect is less pronounced in silk II.[26] In particular, the lowermost shoulder of the carbonyl peak in the silk I form is evident at 176 ppm in the hydrate sample (sample 2). On the contrary, the abovementioned peak narrowing is not prominent in the fibroins from *P. c. ricini*. Instead, it is noteworthy that the relative proportion of the β-sheet forms is significantly increased (samples 6 and 8) as compared with that of the corresponding anhydrous sample (samples 5 and 7, respectively) as a result of hydration.

Figure 5 summarizes $^{13}C$ NMR spectra of conformational transition of lyophilized fibroin immersed in organic solvent for 1 week. The relative proportion of the peaks characteristic of the silk II form is increased at the expense of the peaks marked by silk I that include the "random coil" form. Such conformational transition was accelerated (30 min) when an aqueous solution or fibroin gel was used as starting material (spectra not shown). The achieved conformational transitions thus obtained were demonstrated by the bar graph in Figure 6.[27] The silk II content thus obtained is 12–74%. It is interesting to

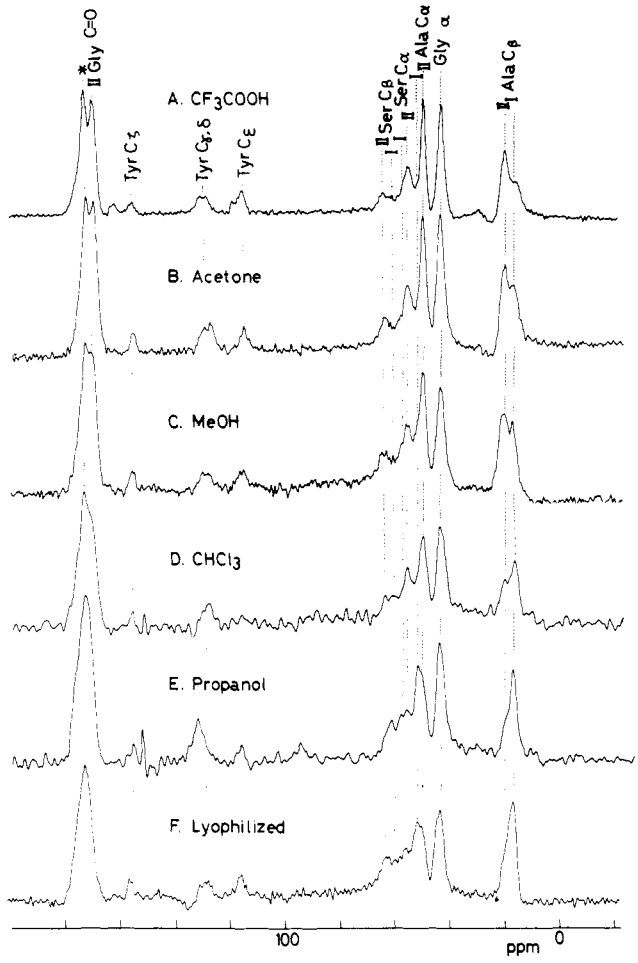


**Figure 5.** Solvent-induced $^{13}C$ NMR spectral change of lyophilized fibroin from *B. mori*. $^{13}C$ NMR spectrum of the lyophilized sample prior to the any treatment is shown in Figure 5F for the sake of comparison.

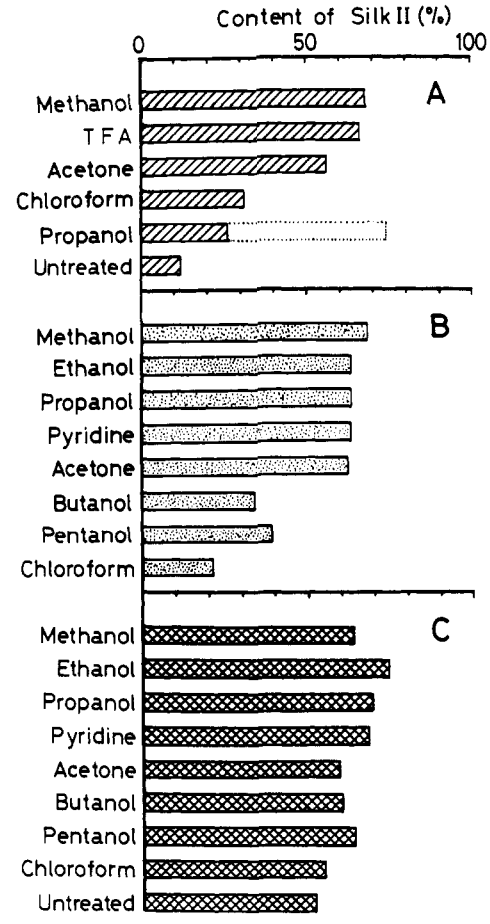


**Figure 6.** Graphical representation of the silk II content induced by solvent treatment. The data presented (±15%) were obtained by examination of the relative peak intensities of Ala $C_\beta$ signals between peaks I and II, with the aid of curve fitting by assuming Gaussian line shape. Starting materials: (A) lyophilized fibroin, (B) regenerated fibroin solution, and (C) fibroin gel. The dotted bar graph indicates that the data were taken in the presence of 50% water as the solvent.

note that conformational transition is enhanced when water molecules are present in the solvent of the lyophilized sample (50% aqueous solution) (Figure 6A). On the contrary, the solvent used in this study did not induce any prominent conformational transition of fibroin gel because the maximal conformational transition was almost already achieved at the occasion of gel formation.

Figures 7 and 8 summarize the spectral change of $^{13}C$ NMR spectra of *B. mori* and *P. c. ricini* fibroins caused by compression, drawing, or hydration. The effect of hydration followed by drying is less pronounced but significant (Figures 7C and 8D) as compared with that of the above-mentioned hydration-induced conformational change (15–45 h) (see Figures 3–5). Compression (at 560 kg/cm$^2$) did not affect any spectral change for both types of fibroins (Figures 7A and 8C). On the other hand, drawing caused significant spectral change in both samples but in a different manner. Drawing induced considerable broadening of peaks in *B. mori* (Figure 7B). However, drawing increased to a similar extent the $\beta$-sheet form in the case of *P. c. ricini* fibroin (Figure 8B) as that obtained by immersing the sample in methanol (Figure 8A).

## Discussion

**Conformational Characterization by $^{13}C$ NMR.** Figure 1 shows that the $^{13}C$ NMR spectrum of the silk I form from the Cp fraction of *B. mori* silk fibroin is well resolved: in particular, the carbonyl $^{13}C$ NMR signals are split into three peaks depending on the variety of amino acid residues involved. However, such a peak splitting is obscured for cast or lyophilized fibroins, as starting materials of the conformational transition, although the rest is very similar between these fibroins and silk I samples (Figures 3 and 5). Such unresolved carbonyl peaks arose from the superposition of $^{13}C$ NMR signals from segments, other than the central Cp domain, whose respective ($\phi$, $\psi$) torsion angles are distorted to some extent from those of the standard silk I form. This situation could be extended to the region adopting the "random coil" conformation as viewed from X-ray diffraction and infrared spectroscopy. As pointed out already, the "random coil" conformation in the solid state is not always completely amorphous as shown by the ensemble of frozen allowed conformers present in solution because observed $^{13}C$ NMR signals are not as broadened as expected from the sum of the peaks of all allowed conformations (5–10 ppm).[14] Instead, it is reasonable to consider, on the basis of the similarity of $^{13}C$ chemical shifts between silk I and "random coil" forms,[13] that the "random coil" conformation is a silk I type in which the crystalline packing is distorted to some extent by the presence of conformers and/or segments in which the torsion angles deviate slightly from those of the normal silk I form.[14]

It appears from Figure 2A that almost all Ala residues in the cast film of *P. c. ricini* silk fibroin participated in the domains of the $\alpha$-helix conformation, as judged by

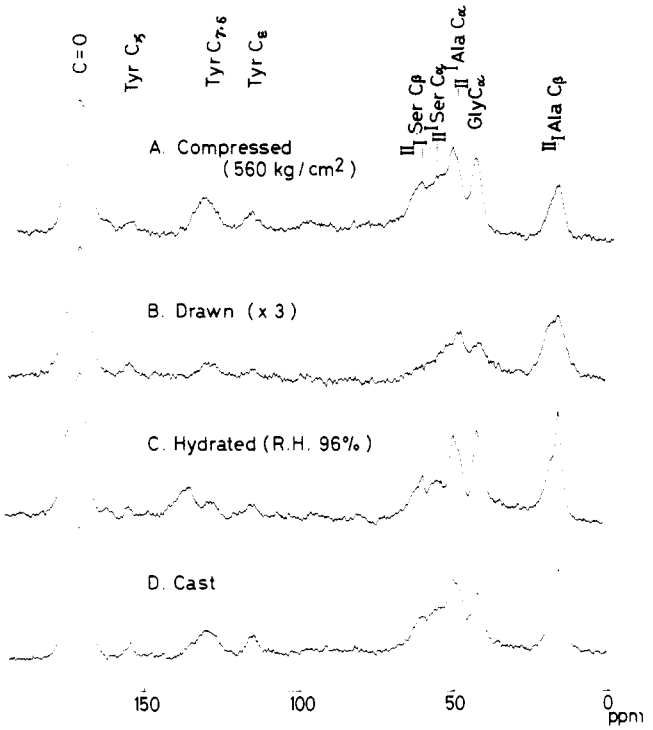


**Figure 7.** $^{13}C$ NMR spectral change of cast film (D) from *B. mori* fibroin after hydration (96% RH; 1 week) (C) and mechanical treatment after hydration of 30 min at 96% RH (A and B). These hydrate samples were dried in vacuo before measurements.

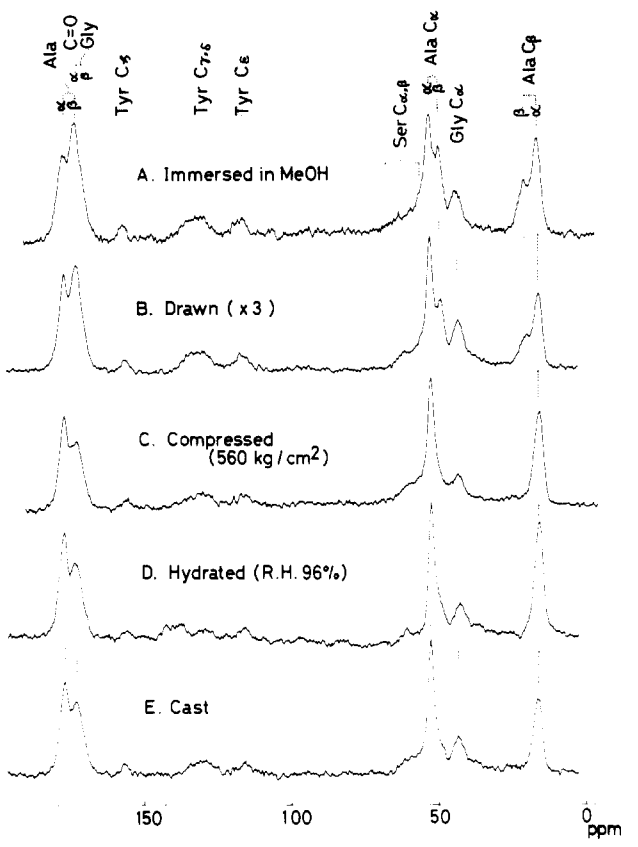


**Figure 8.** $^{13}C$ NMR spectral change of cast film (E) from *P. c. ricini* fibroin after hydration (96% RH; 1 week) (D) and mechanical treatment after hydration of 30 min at RH 96% (B and C). A spectral change induced by immersing in methanol was shown (A). These hydrate samples were dried in vacuo before measurements.

the conformation-dependent $^{13}C$ chemical shifts of the $C_\alpha$, $C_\beta$, and C=O carbons of the Ala residue.[15-17] In fact, the $\alpha$-helix content is almost 100% as viewed from the peak profile of the $C_\beta$ signal, although the Ala $C_\alpha$ signal has the less intense tail (ca. 13%) at the position of the $\beta$-sheet form. In addition, it is estimated, from the relative peak intensities of Gly C=O peaks taking $\alpha$-helix and $\beta$-sheet forms[28] (Figure 2A), that roughly 50% of total Gly residue is involved in the domain of the abovementioned $\alpha$-helix conformation. Therefore, the $\alpha$-helical content in the cast film from *P. c. ricini* is roughly estimated as 65%, from the relative proportion of amino acid residues involved in the $\alpha$-helix (48% Ala + 0.5 × 33% Gly).[29] This estimated $\alpha$-helix content is much higher than that obtained from the data of an aqueous solution at 0 °C (26%).[30] In that case, only 78% of the Ala residues are involved in $\alpha$-helix. This obvious discrepancy of $\alpha$-helical content between aqueous solution and the solid state could be compromised by taking into account the existence of two types of $\alpha$-helical domains: stable and less stable domains in the solid state.

Asakura et al.[30] previously showed that segments of $-(Ala)_n-$ sequence with an average residue number, 22, participated in the stable $\alpha$-helix domain in aqueous solution. Saitô et al. showed that $(Ala)_n$ with $n = 16$ is able to form the $\alpha$-helix in the solid state.[31] In addition, it was previously demonstrated[22,32] that a smaller amount of the Gly residue (5–13%) as a guest molecule could be virtually incorporated into the $\alpha$-helices of host polypeptides in a random copolymer such as $(Ala,Gly)_n$ in spite of the Gly residue being known as a strong helix breaker.[33] This is not unexpected because the local $\alpha$-helical conformation at the Gly residue is stabilized when this residue is sandwiched by the helix-forming Ala residue. In fact, these findings suggest that segments of a shorter alanine sequence, $-(Ala)_m-Gly-(Ala)_n-$ ($m + n$ = 7–20), can form an $\alpha$-helical conformation in the cast film of *P. c. ricini* fibroin. Therefore, it is concluded that the less stable $\alpha$-helices in *P. c. ricini* fibroin in the solid are straightforwardly ascribed to domains with the abovementioned sequence, $-(Ala)_m-Gly-(Ala)_n-$ ($m + n \geq 7$).[34] Obviously, the $\alpha$-helix conformation of this domain is less stable in the hydrophilic environment and is easily susceptible to hydration-induced conformational change, as described later.

**The Effect of Hydration.** It is noteworthy that hydration caused significant spectral change in the cast films of *B. mori* and *P. c. ricini* fibroins in a different manner (Figures 3 and 4): peak narrowing and conformational change for the former and the latter, respectively. In particular, $^{13}C$ NMR line widths were substantially narrowed (Ala $C_\alpha$ and $C_\beta$ and Ser $C_\alpha$ and $C_\beta$ signals of the silk I form) by hydration of the cast film as compared with those of anhydrous samples. In other words, the former and the latter effects can be visualized as hydration-induced conformational change of smaller and larger amplitude of torsion angles, respectively. Such hydration-induced peak narrowing or spectral changes were also observed for a number of polysaccharide samples.[35-37]

Clearly, the peak narrowing by hydration is explained in terms of conformational readjustment of deformed structures with the aid of hydration because narrowed peaks arose generally from samples of better crystalline packing. Actually, insolubilization of water-soluble *B. mori* silk fibroin membrane occurs when the membrane was kept under 96% RH for 1 day.[20] The "random coil" form is thus stabilized by hydration to yield the silk I form. It

appears, however, that such a hydration-induced conformational stabilization of the silk I form cannot be simply explained in terms of the well-known crank-shaft model.[38] Instead, Asakura and Yamaguchi[39] proposed three models of the silk I form on the basis of solid-state $^{13}C$ NMR spectroscopy, long-range C–H spin coupling, X-ray diffraction patterns, and a conformational calculation taking into account the hydration effect.[40] In any case, a primary site for hydration should be at Ser $O_\gamma$ of the Ser residue (12.2%)[29] because of the presence of free hydroxymethyl groups. The subsequent conformational readjustment or change seem to account well for our view that the "random coil" form is a silk I type conformation. Other plausible sites for hydration may be at residues with a hydrophilic side chain such as Tyr (4.8%), Asp (1.9%), and Glu (1.4%).[29] On the contrary, hydration caused partial conformational change of *P. c. ricini* fibroin from the less stable domain of the $\alpha$-helix to the $\beta$-sheet form (ca. 27 and 20% conversion from the $\alpha$-helix to the $\beta$-sheet forms for samples 6 and 8, respectively). It is now clear that such conformational change would be triggered by destabilization of the local $\alpha$-helical conformation of the Gly residue sandwiched by Ala sequences.

**Solvent-Induced Conformational Transition.** As far as the lyophilized fibroin sample is utilized as a starting material, a polar solvent such as $CF_3COOH$, acetone, or methanol induced a considerable proportion of the conformational transition from the "random coil" or silk I type form to the silk II form. On the contrary, a solvent of lower polarity like chloroform or propanol produced a less pronounced effect (Figures 5 and 6). Thus, it seems that the extent of solvent-induced conformational change is related to the ease of the hydration/dehydration process by these solvents. In fact, a solvent that is freely miscible with water molecules caused the maximal conformational transition, whereas a solvent not miscible with water did not induce any appreciable effect. As pointed out already, hydration of *B. mori* fibroin stabilizes the silk I or silk I type form. On the contrary, it is expected that dehydration by an organic solvent destabilizes the silk I form to result in formation of the silk II form. The rate-determining step in the conformational transition of lyophilized fibroin is thus considered to be a diffusion process of solvent molecules into the individual sites of the molecular chains. Fibroin gel, on the other hand, is not sensitive to treatment of any solvents because the maximal conformational transition due to dehydration is already initiated by the gel formation step. Thus, it is possible to control the conformational character through silk II content by changing the kinds of the organic solvents used. This is useful in the molecular design of the enzyme-immobilized silk fibroin membrane.

**Mechanical Treatment.** As pointed out, hydration stabilized the silk I form. The resulting stabilized conformation could be partially retained, even if such samples were dried in vacuo overnight (Figure 7C). Compression at 560 kg/cm$^2$ was ineffective to conformational transition for both types of fibroins because the pressure employed is too low to induce any conformational transition (Figures 7 and 8). Drawing, on the other hand, was found to be effective in inducing conformational change for both fibroins, although the effect to *P. c. ricini* fibroin is more remarkable. Again, the presence of the less stable $\alpha$-helix, as discussed in the previous section, is responsible for the initiation of this transition. Drawing of *B. mori* fibroin does not always produce a sample of better molecular orientation, as viewed from the $^{13}C$ NMR line widths (Figure 7). It should be noted that these insolubilization methods of the water-soluble membrane were used for the purpose of enzyme immobilization, but the conformational character of these membranes after such a treatment is different considerably among them.

## Concluding Remarks

We analyzed the manner of conformational change of fibroin samples, from the silk I or $\alpha$-helix form to the silk II or $\beta$-sheet form, respectively, as produced by hydration or solvent or mechanical treatment and analyzed by high-resolution solid-state $^{13}C$ NMR spectroscopy. We found that this approach is most appropriate for the quantitative evaluation of the proportion of individual forms. The present NMR data clearly showed that hydration causes conformational readjustment of the distorted silk I type form, leading to the silk I form. In any case, it is found that the hydration or dehydration process plays a dominant role in the conformational transition as expected from the natural process of silkworms. Quantitative evaluation of the relative proportion of conformational feature in silk fibroin can be successfully performed by the high-resolution $^{13}C$ NMR method, as a means for the setup of entrapment of enzymes utilizing fibroin, together with a gentle treatment such as solvent or mechanical treatment.

## References and Notes


(1) Lucas, F.; Rudall, K. M. In *Comprehensive Biochemistry*; Florkin, M., Scotz, E., Ed.; Elsevier: Amsterdam, 1968; Vol. 26B, Chapter 7.
(2) Fraser, R. D. B.; MacRae, T. P. In *Conformation of Fibrous Proteins and Related Synthetic* Polypeptides; Academic Press: New York, 1973; Chapter 13.
(3) Lotz, B.; Cesari, F. C. *Biochimie* **1979**, *61*, 205.
(4) Hojo, N., Ed. *Zoku Kenshi no Kozo* (*Structure of Silk Fibers*); Shinshu University: Ueda, Japan, 1980.
(5) Hirabayashi, K.; Ishikawa, H.; Kasai, N.; Kakudo, M. *Kogyo Kagaku Zashi* **1970**, *73*, 1381.
(6) Magoshi, J. *Kobunshi Ronbunshu* **1974**, *31*, 765.
(7) Magoshi, J.; Magoshi, Y.; Nakamura, S. *J. Appl. Polym. Sci.; Appl. Polym. Symp.* **1985**, *41*, 187.
(8) Asakura, T. *Bioindustry* **1987**, *4*, 36.
(9) Kuzuhara, A.; Asakura, T.; Tomoda, R.; Matsunaga, T. *J. Biotechnol.* **1987**, *5*, 207.
(10) Asakura, T.; Yoshimizu, H.; Kuzuhara, A.; Matsunaga, T. *Nippon Sanshigaku Zasshi* **1988**, *57*, 203.
(11) Demura, M.; Asakura, T. *Biotechnol. Bioeng.* **1989**, *33*, 598.
(12) Saitô, H.; Iwanaga, Y.; Tabeta, R.; Narita, M.; Asakura, T. *Chem .Lett.* **1983**, 427.
(13) Saitô, H.; Tabeta, R.; Asakura, T.; Iwanaga, Y.; Shoji, A.; Ozaki, T.; Ando, I. *Macromolecules* **1984**, *17*, 1405.
(14) Asakura, T.; Kuzuhara, A.; Tabeta, R.; Saitô, H. *Macromolecules* **1985**, *18*, 1841.
(15) Saitô, H.; Tabeta, R.; Shoji, A.; Ozaki, T.; Ando, I.; Asakura, T. In *Magnetic Resonance in Biology and Medicine*; Govil, G., Kheterapal, C. L., Saran, A., Eds.; Tata McGraw-Hill: New Delhi, 1985; pp 195–215.
(16) Saitô, H. *Magn. Reson. Chem.* **1986**, *24*, 835.
(17) Saitô, H.; Ando, I. *Annu. Rep. NMR Spectrosc.* **1989**, *21*, 209.
(18) Saitô, H.; Ishida, M.; Yokoi, M.; Asakura, T. *Macromolecules*, preceding paper in this issue.
(19) Asakura, T.; Watanabe, Y.; Itoh, T. *Macromolecules* **1984**, *17*, 2421.
(20) Demura, M.; Asakura, T.; Kuroo, T. *Biosensor*, in press.
(21) The amount of water taken up during hydration is typically 52.4 and 53.3% for the silk I and silk II samples, respectively.[20]
(22) Asakura, T.; Hirano, K.; Takatsu, R., unpublished results.
(23) Kricheldorf, H. R.; Muller, D.; Ziegler, D. *Polym. Bull. (Berlin)* **1983**, *9*, 284.
(24) Saitô, H.; Tabeta, R.; Kuzuhara, A.; Asakura, T. *Bull. Chem. Soc. Jpn.* **1986**, *59*, 3383.
(25) A low intense peak at 130 ppm is ascribed to the residual spinning sideband still persistent in spite of the use of the TOSS pulse sequence because aromatic $^{13}C$ signals should be reduced in the Cp fraction.

(26) Horii, F.; Hirai, A.; Kitamaru, R. *Proceedings of 24th NMR Symposium, Japan*; Tsukuba, 1985; pp 155-158.
(27) The procedure of curve-fitting was previously described[14] (see caption to Figure 6). A plot of the relative peak intensities against the contact time gave straight lines with almost equal gradients corresponding to equal proton spin-lattice relaxation times of the rotating frame after 1 ms (Ishida, M. MS thesis, Tokyo University of Agriculture and Technology, 1989).
(28) It was shown from the curve-fitting procedure on the carbonyl peak of *P. c. ricini* fibroin (Figure 2A) that the relative peak intensities of Ala, Gly ($\alpha$-helix) and other residues, and Gly ($\beta$-sheet) C=O peaks are 50%, 32%, and 18%, respectively. Therefore, the peak intensity of Gly ($\alpha$-helix) is estimated as 15% by substracting 18% (the Gly residue adopting the $\beta$-sheet form) from the total Gly content (33%). Then, the Ala/Gly ratio involved in the $\alpha$-helix is approximately estimated as 3.3.
(29) Shimura, K. In *Zoku Kenshi no Kozo (Structure of Silk Fibers)*; Hojo, N., Ed.; Shinshu University: Ueda, Japan, 1980.
(30) Asakura, T.; Kashiba, H.; Yoshimizu, H. *Macromolecules* **1988**, *21*, 644.
(31) Saitô, H.; Tabeta, R.; Shoji, A.; Ozaki, T.; Ando, I. *Macromolecules* **1983**, *16*, 1050.
(32) Ando, S.; Yamanobe, T.; Ando, I.; Shoji, A.; Ozaki, T.; Tabeta, R.; Saitô, H. *J. Am. Chem. Soc.* **1985**, *107*, 7648.
(33) Chou, P. Y.; Fasman, G. *Biochemistry* **1974**, *13*, 222.
(34) This condition still accounts for 50% of the total Gly residues involved in the $\alpha$-helix, in view of the observed Ala/Gly ratio in the $\alpha$-helix of the fibroin sample is approximately 3.3 (see footnote 28). However, it is more provable that the Gly residue can be incorporated into $\alpha$-helical segments of a Ala sequence shorter than seven as mentioned above. In fact, Chou and Fasman showed that $\alpha$-helix nucleation occurs when four helical residues are located out of six residues along the polypeptide chain.[33]
(35) Marchessault, R. H.; Taylor, M. G.; Fyfe, C. A.; Veregin, R. P. *Carbohydr. Res.* **1985**, *144*, C1.
(36) Horii, F.; Hirai, A.; Kitamaru, R. *Macromolecules* **1986**, *19*, 930.
(37) Saitô, H.; Yokoi, M.; Yoshioka, Y. *Macromolecules* **1989**, *22*, 3892.
(38) Lotz, B.; Keith, H. D. *J. Mol. Biol.* **1971**, *61*, 195.
(39) Asakura, T.; Yamaguchi, T. *J. Seric. Sci. Jpn.* **1987**, *56*, 300.
(40) Hodes, Z. I.; Nemethy, G.; Sheraga, H. A. *Biopolymers* **1979**, *18*, 1565.

# Cross-Linking Reactions in Maleimide and Bis(maleimide) Polymers. An ESR Study

**I. M. Brown* and T. C. Sandreczki**

*McDonnell Douglas Research Laboratories, St. Louis, Missouri 63166.*
*Received April 18, 1989; Revised Manuscript Received June 7, 1989*

ABSTRACT: The results of electron spin resonance (ESR) measurements on the homopolymerization reactions of two bis(maleimides) and several maleimide model compounds containing different amounts of radical initiators (0–10 wt %) are reported. Two types of radicals were identified: the propagating radical, which is an intermediate in the chain growth polymerization, and species such as the bis(maleimidophenyl)methyl radical and a substituted vinyl radical, both of which are the result of hydrogen atom abstraction reactions. The concentrations of the radicals observed in the hot-melt homopolymerization of one particular bis(maleimide) were determined as a function of cure time from the integrated ESR intensities. The similarity of the ESR results obtained in air-curing and in vacuum-curing suggests that hydroperoxides, which might be formed by reactions with ambient oxygen during the cure process, play no role as radical initiators. On the other hand, differential scanning calorimetry, along with ESR, suggests that trace amounts of impurities act as radical initiators; but, even in the absence of impurities, the bis(maleimides) will still homopolymerize by direct thermal homolysis. There is also evidence for thermal as well as thermooxidative degradation.

## Introduction

Cured carbon fiber/bis(maleimide) composites are high-modulus, high-strength materials that are better than carbon fiber/epoxy composites in retaining their mechanical properties after hot-wet or hot-dry exposures at 525 K.[1-5] One undesirable property of bis(maleimide) matrices, however, is that they are brittle. Since the cross-link density of the network determines the strength and fracture toughness of the matrix, it is important to understand the mechanisms of the cross-linking reactions and to find ways of controlling these reactions. We are using electron spin resonance (ESR) spectroscopy to investigate these cross-linking reactions because they involve a free-radical mechanism. In this paper we report on our studies of the types and concentrations of radicals formed and trapped in the polymer matrix when bis(maleimide) monomers and selected maleimide model compounds undergo homopolymerization in the presence of different amounts of free-radical intitiator (0–10 wt %). The bis(maleimides) studied were 4,4′-bis(maleimidophenyl)-methane (BDM) and the research-grade monomer 6-maleimido-1-(4′-maleimidophenyl)-1,3,3-trimethylindane (CIBA). The maleimides included in this study were *N*-phenylmaleimide, *N*-methylmaleimide, and maleimide. The structures are shown in Figure 1.

## Experimental Section

The BDM monomer, the main bis(maleimide) used in many commercial resin formulations, was purified by recrystallization from hot mixtures of chloroform and methanol. Small quantities of the material were also purified with high-pressure liquid chromatography using a silica gel column as the stationary phase and methylene chloride containing 0.2% methanol as the mobile phase. The CIBA bis(maleimide) was used as received from the Ciba Geigy Chemical Co., Ardsley, NY. The BDM monomer and the maleimide monomers were obtained from the Aldrich Chemical Co., Milwaukee, WI. The latter were purified either by vacuum sublimation or by recrystallization from suitable solvents. The deuterated material *N*-phenyl-2,3-$d_2$-

0024-9297/90/2223-0094$02.50/0 